International Journal of Pharmaceutics: X 1 (2019) 100037

Contents lists available at ScienceDirect

International Journal of Pharmaceutics: X

journal homepage: www.journals.elsevier.com/international-journal-of-pharmaceutics-x

Atypical compaction behaviour of disordered lactose explained by a shift in type of compact fracture pattern

Samaneh Pazesh*, Ann-Sofie Persson, Göran Alderborn

Department of Pharmacy, Uppsala University, Box 580, SE-751 23 Uppsala, Sweden

ARTICLE INFO

Keywords:
Lactose
Tensile strength
Compaction pressure
Porosity
Core-shell particles
Tablet fracture

ABSTRACT

The objective was to investigate tabletability and compactibility for compacts of a series of α-lactose monohydrate powders with different degree of disorder. Regarding the tabletability, the powders of high degree of disorder displayed similar behaviour that deviated markedly from the behaviour of the crystalline powders and the milled powder of modest degree of disorder. The Ryshkewitch-Duckworth equation, describing compactibility, was nearly linear for the crystalline powders, while for the disordered powders the model failed to describe the relationships, i.e. the disordered powders were characterised by a plateau in the Ryshkewitch-Duckworth plots over a relatively wide range of compact porosities. It was concluded that the difference in compaction behaviour of the milled particles compared to the crystalline powders was primarily explained by the increased particle plasticity of the disordered particles. The plateau in the Ryshkewitch-Duckworth plots obtained for the disordered powders was explained by a change in the fracture behaviour of the compacts, from an around grain to an across grain fracture pattern. This implied that the disordered particles can be described as a type of core-shell particles with an amorphous shell and a defective crystalline core.

1. Introduction

According to the bond summation concept, the tensile strength of a compact is controlled by two factors, i.e. the inter-particulate bonding (or adhesion) strength and the inter-particulate specific contact area (contact area per cross-sectional area of compact) (Alderborn and Nyström, 1982) and their relative contribution to the tensile strength has been discussed in the literature (Nyström et al., 1993; Osei-Yeboah et al., 2016). The evolution in inter-particulate specific contact area during powder compaction is affected by the physical properties of the particles, including their plastic stiffness and brittleness (Nyström et al., 1993; Sun, 2011). It is proposed (Sebhatu and Alderborn, 1999; Sun, 2011) that a decreased particle plastic stiffness (an increased particle plasticity) will provide condition for the formation of larger areas of inter-particulate contact and thus a higher compact forming ability of the powder.

It is commonly acknowledged that fully amorphous particles prepared by spray-drying may show improved compact forming ability compared to a crystalline particle of the same compound, e.g. (Sebhatu and Alderborn, 1999; Vromans et al., 1987). One practical use of this phenomenon is that special grades of lactose that consist of both crystalline and amorphous lactose have been developed. An explanation for the superior compact forming ability of the amorphous form compared to the crystalline is a difference in their particle plasticity (Sebhatu and Alderborn, 1999). We have recently shown (Pazesh et al., 2018) that the particle plastic stiffness of milled α-lactose monohydrate particles decreases with an increased degree of particle disorder and it may therefore be hypothesised that particle disordering will create opportunity for an increased compact forming ability of lactose particles. The milling may however not only change the particle plastic stiffness but also the nature of the particle surface in terms of its rugosity, deformability and surface energy, properties that may affect the particle-particle bonding strength and not only the area of intimate contact. Thus, milling may affect the compact forming ability by affecting both the particle plastic stiffness and the particle-particle bonding strength.

The physical nature of mechanically disordered particles has been the object of considerable discussion in the literature and it is proposed (Dujardin et al., 2013; Luisi et al., 2012; Newman and Zografi, 2014) that they may be composed of crystallites surrounded by crystal defects (one-state model) or consist of amorphous and crystalline domains (two-state model) or a combination thereof. By studying lactose particles partially disordered by milling, we reported (Badal Tejedor et al., 2017) that the particles had a surface which approximated the nature of the surface of fully amorphous particles prepared by spray-drying. The milled lactose particles could hence be described as a type of core-shell particles with a partially disordered core with defects and an

* Corresponding author.
E-mail address: samaneh.pazesh@farmaci.uu.se (S. Pazesh).

https://doi.org/10.1016/j.ijpx.2019.100037
Received 9 July 2019; Received in revised form 26 September 2019; Accepted 1 October 2019
Available online 08 November 2019

amorphous shell, i.e. a two-state model (Bordet et al., 2016). In this paper, the compaction behaviour of this type of disordered core-shell lactose particles is investigated. We thus now ask the question if both the total degree and the distribution of disordered solid is of importance for the compaction behaviour of disordered particles or if the compaction behaviour is controlled only by the degree of disordered solid, similar to the compressibility (Pazesh et al., 2018). The term compaction behaviour is here used as a collective term of how the compact tensile strength evolves with reduced compact porosity (sometimes referred to as compactibility (Tye et al., 2005)) or with increased compaction pressure (sometimes referred to as tabletability (Tye et al., 2005)). Thus, the objective of this paper is to investigate the compactibility and the tabletability for compacts of a series of α-lactose monohydrate powders with different degree of disorder.

2. Materials and methods

2.1. Materials

Crystalline α-lactose monohydrate of two particle sizes Pharmatose® 200 M and Lactohale® LH300, hereafter denoted CL200 and LH300, were supplied by DFE Pharma, the Netherlands. Magnesium stearate (Sigma-Aldrich, Sweden) was used as a lubricant. Magnesium chloride ($MgCl_2$) and phosphorus pentoxide (P_2O_5) were used as desiccator salts and were purchased from Sigma-Aldrich, Sweden and VWR, Sweden, respectively.

2.2. Preparation of powders

Fully amorphous lactose (as previously shown in (Pazesh et al., 2018)) was prepared by dissolving CL200 in deionised water at a solid concentration of 10% (w/w) and agitated for at least 15 h before spray-drying. The spray-drying (Mini spray dryer B-290, Büchi Labortechnik AG, Flawil, Switzerland) was conducted at an inlet temperature of 155 °C and an outlet temperature of 85 °C. The solution was fed to the spray-drier at a rate of ~ 4 mL/min with a peristaltic pump. The aspirator was set to 100% and the flow meter (compressed air) to 40 mL/min. The spray-dried lactose powder is henceforth denoted SDL.

Milled lactose powders were prepared by milling approximately 1 g of CL200 for 60, 300, and 1200 min in a planetary ball mill (PM 100 CM, Retsch, Germany). The milling was performed at a rate of 400 rpm in a 12 cm^3 stainless steel milling jar with 50 stainless steel spherical balls of 5 mm diameter, i.e. a ball-to-powder mass ratio of 25:1 was used during milling. In order to cool the jar and thus minimise heating of the sample, a pause period of 5 min was employed every 20 min of milling. The milling was performed in an environmentally controlled room at 30 ± 5% relative humidity (RH) and 22 ± 3 °C. Henceforth, the milled powders are denoted ML60, ML300, and ML1200 where the numbers indicate the respective milling times in minutes.

2.3. Powder compaction

The CL200, LH300, SDL and ML powders were stored for at least two days prior to compaction in desiccators over P_2O_5 or over a saturated solution of $MgCl_2$ giving a RH of ~ 0% and ~ 33%, respectively. Approximately 400 mg powder was compacted at a rate of 10 mm/min using a materials tester (Zwick Z100, Zwick/Roell GmbH & Co, Ulm, Germany) equipped with 11.3 mm diameter flat-faced circular punches. The lower punch was stationary during compaction and compaction pressures of 10, 20, 50, 100, 200, 300, and 500 MPa were applied.

CL200, LH300, and ML60 powders were also compacted at compaction pressures of 900 and 1200 MPa. These powders were compacted in a single-punch press (Korsch EK0, Germany) using flat-faced punches with a diameter of 5.65 mm. The minimum punch separation distance was kept constant in all these compaction experiments and the compaction pressure was regulated by the amount of powder filled in die. The minimum punch separation distance was obtained by placing a metal stub of 2 mm height in-between the punches and the separation distance was regulated until a pressure of 5 MPa was generated on the upper punch.

For all powders, five compacts were compacted at each compaction pressure. The punches and the die were lubricated using 1% magnesium stearate in ethanol (95% w/w) prior die-filling. The compaction experiments were performed in a humidity controlled room at 30 ± 5% RH and at 22 ± 3 °C.

2.4. Compact properties

2.4.1. Apparent amorphous content

The apparent amorphous content (AAC) of each compact was quantified directly after compaction with Raman spectroscopy as described previously (Pazesh et al., 2016). Raman spectra were obtained using Raman Ewave Opetronics Inc. (SLSR-ProTT analyser, Irvine, CA, USA), equipped with TE cooled CCD detector and a laser source operating at an excitation wavelength of 785 nm. The baseline of the Raman spectra was corrected and normalised using a straight baseline approach and the quantification was performed using principal component analysis (PCA).

2.4.2. Tensile strength and porosity

The compact dimensions (height h_i and diameter d_t) were measured using Litematic VL 50A, Mitutoyo, Japan. The compact tensile strength (σ_t) was then calculated according to (Fell and Newton, 1970):

$$\sigma_t = \frac{2F_t}{\pi h_i d_t}, \tag{1}$$

where F_t is the radial compact fracture force measured by a hardness tester (PharmaTest, PTB311E, Hainburg, Germany) operating at a rate of 20 N/s.

Additionally, the compact mass and the compact dimensions were used to calculate the compact density (ρ_{comp}) to enable subsequent calculations of out-of-die compact porosity (ε):

$$\varepsilon = 1 - \left(\frac{\rho_{comp}}{\rho_{app}}\right), \tag{2}$$

where ρ_{app} is the apparent particle density. The ρ_{app} of the investigated powders was measured using helium pycnometry and are reported earlier (Pazesh et al., 2018).

2.4.3. Tensile strength-compaction pressure relationships

As descriptors of the compact tensile strength-compaction pressure relationship, three compaction parameters, namely P_{c1}, P_{c2}, and Γ, were derived (Alderborn, 2003; Persson and Alderborn, 2018). P_{c1} is the threshold pressure at which a compact forms, P_{c2} is the threshold pressure at which the maximum tensile strength ($\sigma_{t,\,max}$) is reached, and Γ is a particle plasticity parameter (Persson and Alderborn, 2018).

The P_{c1} parameter was determined by extrapolating the tensile strength-compaction pressure relationship in the compaction pressure range 10–100 MPa using linear regression ($R^2 > 0.9664$). Additionally, the slope of the tensile strength-compaction pressure profile (k_c) was calculated by linear regression using the same pressure range.

The P_{c2} parameter was calculated by extrapolating the linear regression curve obtained from the tensile strength-compaction pressure relationship to the $\sigma_{t,\,max}$ in the compaction pressure range 10–100 MPa according to:

$$P_{c2} = \frac{\sigma_{t,max} - y_{intercept}}{k_c}. \tag{3}$$

The $\sigma_{t,\,max}$ was approximated using the average σ_t of the two to three highest compaction pressures where a plateau could be identified (Figs. 1A and B).

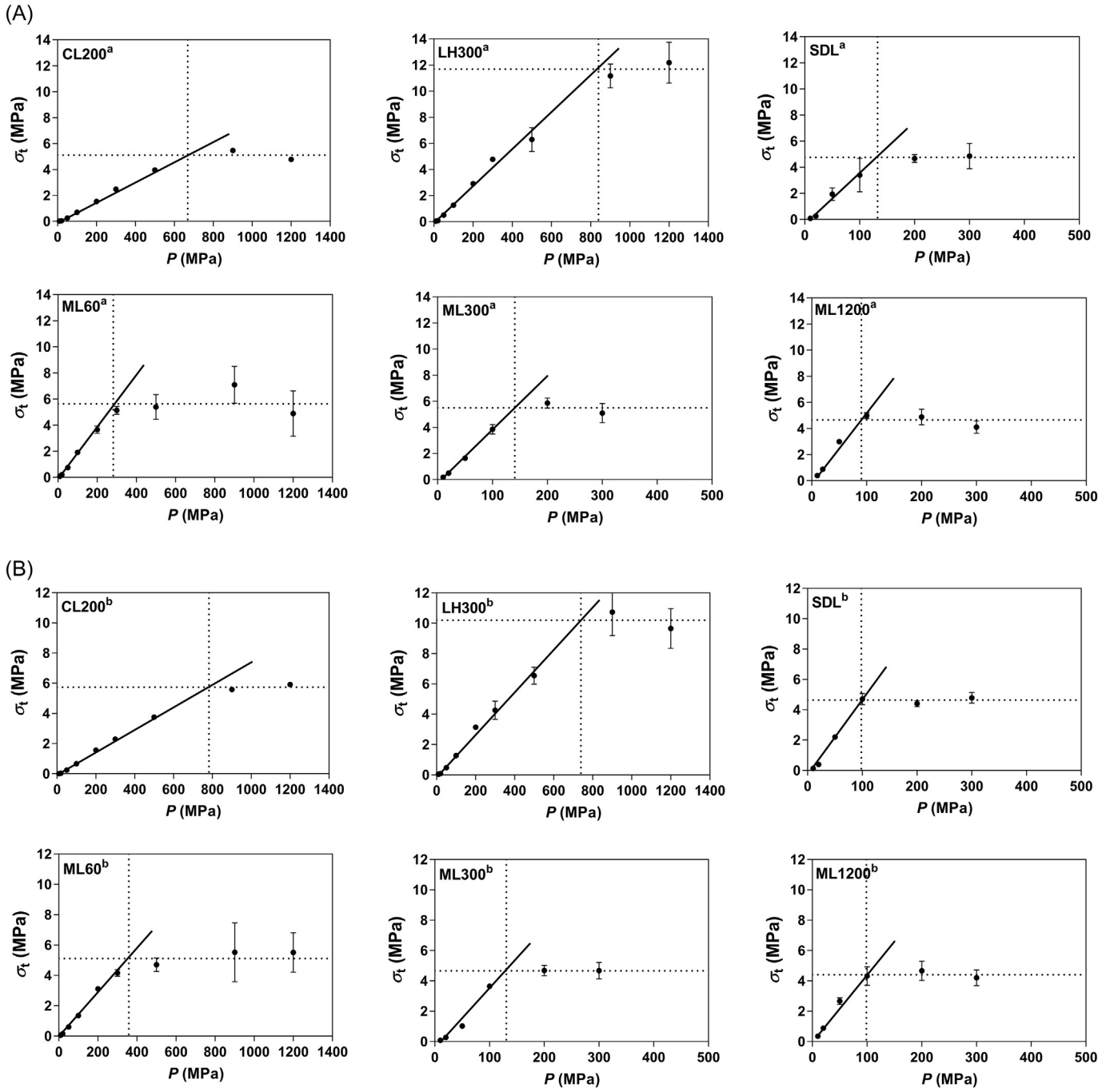

Fig. 1. The tensile strength (σ_t) and compaction pressure (P) relationship of crystalline lactose CL200, crystalline lactose LH300, lactose milled for 60 min (ML60), lactose milled for 300 min (ML300), lactose milled for 1200 min (ML1200) and spray-dried lactose (SDL). Powder was pre-stored at 0% RH.(A) and 33% RH (B) prior compaction. The dashed horizontal line represents the maximum tensile strength ($\sigma_{t,\,max}$) and the dashed vertical line represents the pressure at which the $\sigma_{t,\,max}$ is reached. The error bars represent the standard deviations.

The plasticity parameter Γ was calculated as the reciprocal of the slope obtained by linear regression with an R^2-value > 0.9774 of the relative tensile strength $\left(\frac{\sigma_t}{\sigma_{t,max}}\right)$ and the effective applied pressure $(P - P_{c1})$ in the compaction pressure range 10–100 MPa according to (Persson and Alderborn, 2018):

$$\frac{\sigma_t}{\sigma_{t,max}} = \frac{1}{\Gamma}(P - P_{c1}). \quad (4)$$

2.4.4. Tensile strength –porosity relationships

The compact tensile strength-compact porosity relationship was investigated using the Ryshkewitch-Duckworth equation according to (Duckworth, 1953; Ryshkewitch, 1953):

$$\ln\left(\frac{\sigma_t}{\sigma_0}\right) = -k_R \bullet \varepsilon, \quad (5)$$

where σ_t is the compact tensile strength at each compaction pressure, σ_0 is the tensile strength at zero porosity, k_R is a constant, and ε is the compact porosity.

2.4.5. Scanning electron microscopy

Scanning electron microscopy (SEM) images were captured of

compact fragments (obtained after the compact hardness test described in Sec. 2.4.2) compacted from SDL powder at 50, 100, 200, and 300 MPa. The fragment was glued onto a metal cylinder and subsequently sputtered under Argon with Au/Pd in a sputter coater (Polaron, Quorum Technologies Ltd., Newhaven, U.K.). Images of the outer surface and the fracture surface of compact fragments were taken in the scanning electron microscope (Leo (Zeiss), 1550 Schottky, Germany, equipped with SmartSEM software) at an accelerating voltage of 2 kV.

2.5. Statistical analysis

Results are presented as mean values and relative standard deviations in tables. In the figures the results are presented as mean values and the error bars display the standard deviations. Statistical significances have been validated using one-way analysis of variance (ANOVA) test or a *t*-test with the GraphPad Prism 8.1.0 software. The statistical level p was set to 0.05 and $p < 0.05$ was considered as statistically significant.

3. Results

3.1. Degree of disorder

The original lactose powders (CL200 and LH300) were crystalline and the spray-dried powder (SDL) was fully amorphous (Table 1). For the milled powders (ML), the apparent amorphous content (AAC) increased with increased milling time (Table 1). Pre-storage of ML powders in the humid atmosphere (33% RH) gave for compacts of ML60 and ML300 markedly lower AAC than pre-storage in the dry atmosphere (0%) (Table 1).

3.2. Compact tensile strength-compaction pressure relationships

The relationship between compact tensile strength (σ_t) and compaction pressure was generally linear in the pressure dependent region, i.e. σ_t increased approximately linearly with compaction pressure until a tensile strength plateau ($\sigma_{t,\ max}$) was reached (Figs. 1A and B). The $\sigma_{t,\ max}$ was reached at considerably higher compaction pressures for the crystalline lactose powders (700–900 MPa) compared to for the ML and the SDL powders (< 300 MPa).

For the reference powders, $\sigma_{t,\ max}$ was higher for LH300 than for CL200 and SDL (Figs. 1A, B, and 2A). The slope (k_c) of the tensile strength-compaction pressure relationship was also higher for LH300 compared to CL200 (Figs. 1A, B and 2B) explained by their difference in labelled particle size (27.4 µm for CL200 and 3.46 µm for LH300 (Pazesh et al., 2018)). However, the k_c of the amorphous reference (SDL) was higher compared to the crystalline references (Fig. 2B).

The pre-storage humidity had generally a limited influence on both the $\sigma_{t,\ max}$ and the k_c of all reference powders (Figs. 2A and B).

The $\sigma_{t,\ max}$ was statistically the same for the various ML powders (median particle size of ~ 5 µm (Pazesh et al., 2017)) and the amorphous reference SDL and thus the $\sigma_{t,\ max}$ was independent on the degree of disorder (Fig. 2A). Moreover, the $\sigma_{t,\ max}$ of ML powders with low and intermediate degree of AAC (ML60 and ML300) was statistically the same to the $\sigma_{t,\ max}$ of CL200 despite their differences in particle size, i.e. 27.7 µm for CL200, 5 µm for ML60 and ML300 (Pazesh et al., 2017). However, the $\sigma_{t,\ max}$ of LH300 (median particle diameter of 3.46 µm) with similar particle size as ML60 and ML300 (Pazesh et al., 2017) was significantly higher (Fig. 2A). The k_c of ML powders significantly increased with increased degree of disorder, nevertheless the increase was most pronounced from ML60 to ML300 (Fig. 2B). The $\sigma_{t,\ max}$ (Fig. 2A) and the k_c (Fig. 2B) for the ML powders was not influenced when the powder was pre-stored in the humid atmosphere.

By approximating the relationship between σ_t and compaction pressure as consisting of three stages, three compaction parameters could be derived, i.e. P_{c1}, P_{c2}, and Γ. The P_{c1} parameter was generally low for all investigated powders and varied between ~ 1 MPa for powders containing disordered particles to ~ 13 MPa for crystalline lactose powders. Furthermore, the pre-storage humidity had no effect on the P_{c1} parameter.

The P_{c2} parameter varied depending on the physical nature of the particles (Fig. 2C). For the crystalline lactose powders pre-stored at 0% RH, the P_{c2} increased with decreased particle size, i.e. the P_{c2} was higher for LH300 than for CL200. For SDL pre-stored at 0% RH the P_{c2} was significantly lower than the P_{c2} of crystalline lactose powders (Fig. 2C). After storage in the humid environment, the P_{c2} increased for CL200 whereas it decreased for LH300 and SDL (Fig. 2C). Consequently, the P_{c2} for CL200 was similar to LH300 at 33% RH.

For the ML powders, the P_{c2} decreased with an increased degree of disorder (Fig. 2C). For the ML60 with low degree of AAC, the P_{c2} was higher compared to the ML300 and the ML1200 with intermediate and high degree of AAC. However, the P_{c2} of ML60 was significantly lower

Table 1
Degree of disorder of compacts made from original lactose powders, spray-dried lactose and milled lactose pre-stored at 0% RH and 33% RH. The degree of disorder was analysed directly after compaction. Relative standard deviations are given in parentheses (n = 5).

	Degree of disorder (%)								
	10 MPa	20 MPa	50 MPa	100 MPa	200 MPa	300 MPa	500 MPa	900 MPa	1200 MPa
CL200[a]	0	0	0	0	0	0	0	0	0
LH300[a]	0	0	0	0	0	0	0	0	0
ML60[a]	13.2 (0.03)	10.9 (0.02)	7.98 (0.03)	8.69 (0.02)	8.46 (0.01)	8.93 (0.02)	13.5 (0.02)	12.9 (0.06)	11.8 (0.02)
ML300[a]	45.7 (0.02)	46.5 (0.02)	44.0 (0.03)	41.8 (0.01)	41.3 (0.02)	41.1 (0.03)	–	–	–
ML1200[a]	83.1 (0.01)	83.4 (0.01)	82.0 (0.01)	80.5 (0.00)	83.1 (0.00)	79.1 (0.01)	–	–	–
SDL[a]	100 (0.00)	100 (0.00)	100 (0.00)	100 (0.00)	100 (0.01)	100 (0.00)	–	–	–
CL200[b]	0	0	0	0	0	0	0	0	0
LH300[b]	0	0	0	0	0	0	0	0	0
ML60[b]	6.87 (0.01)	7.05 (0.01)	0.69 (0.00)	3.49 (0.01)	1.25 (0.01)	4.89 (0.01)	6.91 (0.01)	8.81 (0.01)	7.89 (0.01)
ML300[b]	24.6 (0.05)	26.4 (0.01)	23.9 (0.01)	38.0 (0.03)	20.3 (0.01)	37.5 (0.02)	–	–	–
ML1200[b]	82.7 (0.01)	83.1 (0.03)	80.3 (0.01)	78.9 (0.01)	80.4 (0.01)	78.0 (0.01)	–	–	–
SDL[b]	99.8 (0.00)	99.3 (0.00)	99.3 (0.00)	100 (0.00)	99.1 (0.00)	99.9 (0.00)	–	–	–

CL200: Crystalline α-lactose monohydrate 200 M.
LH300: Crystalline α-lactose monohydrate LH300.
SDL: Spray- dried lactose.
ML: Milled powder, the numbers are the milling time in minutes.
[a] Powder pre-stored at 0% RH.
[b] Powder pre-stored at 33% RH.

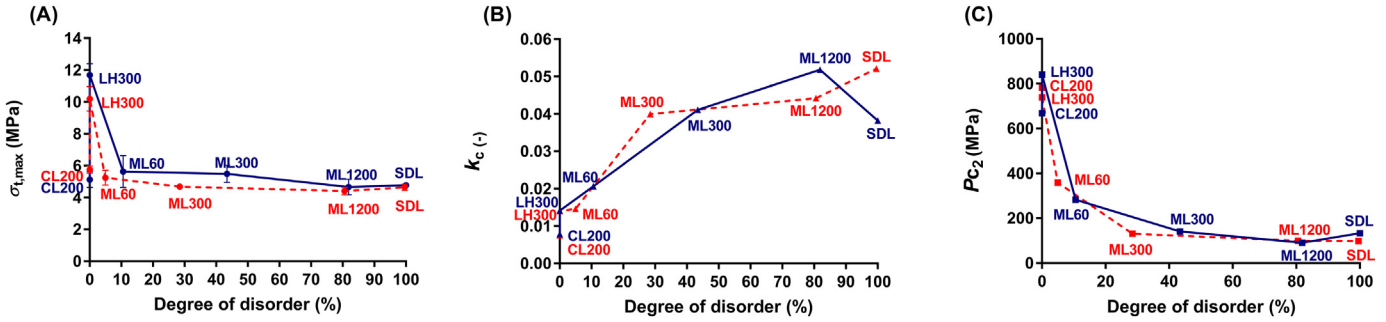

Fig. 2. (A) the maximum tensile strength ($\sigma_{t,\ max}$), (B) the slope of compact tensile strength and compaction pressure relationship profile (k_c) and (C) the second threshold pressure (P_{c2}) as function of degree of disorder. Powder was pre-stored at 0% RH (blue symbol and blue solid line) and at 33% RH (red symbol and red dashed line) prior compaction. The error bars represent the standard deviations. (For interpretation of the references to colour in this figure legend, the reader is referred to the web version of this article.)

than the P_{c2} of crystalline powders. The P_{c2} of ML300 and ML1200 was statistically the same as the P_{c2} of SDL (Fig. 2C). For the ML powders, the pre-storage humidity had minor influence on the P_{c2} despite the occurrence of some recrystallisation of ML60 and ML300 in the humid environment.

The plasticity parameter Γ, i.e. the range of the linear region of the σ_t and compaction pressure relationship, showed similar dependency of the physical nature of the particles as the P_{c2} parameter and hence the results are not presented or discussed further in this study.

3.3. Compact tensile strength-porosity relationships

The relationship between compact tensile strength and porosity (compactibility) was described in accordance with the Ryshkewitch-Duckworth equation. In general, the Ryshkewitch-Duckworth equation was not appropriate to describe the compactibility of the investigated powders (Figs. 3A and B). However, the relationship trend thus obtained was dependent on the physical nature of the particles of investigated powders. For the crystalline lactose powders the relationship was almost linear except at high compact porosity i.e. compacts formed at 10 MPa and 20 MPa. Furthermore, no tensile strength plateau was clearly obtained at low compact porosity for the crystalline powders. For SDL, the relationship was linear at high compact porosities but bended markedly with reduced compact porosity and a tensile strength plateau was clearly obtained at the lowest compact porosities, i.e. below about 18%. For the ML powders, the relationships were more similar to the SDL powder, however the tensile strength plateau of ML60 was obtained at lower compaction porosity, i.e. below about 9% compared to the ML300, ML1200 and SDL. The pre-storage humidity (33% RH) had a small influence on the overall type of relationship for all powders except for CL200 where two linear regions was observed (Figs. 3A and B).

4. Discussion

4.1. Physical nature of investigated particles

The physical nature of partially disordered particles has been the object of considerable discussion in the literature (Bordet et al., 2016; Dujardin et al., 2013; Luisi et al., 2012; Newman and Zografi, 2014; Pazesh et al., 2017) and it has been proposed that they may be composed of crystallites surrounded by crystal defects or alternatively be composed of amorphous and crystalline domains, i.e. a two-phase particle. For the milled lactose particles used in this study we have earlier proposed (Badal Tejedor et al., 2017) that although the milled particles were only partially disordered, their surface approximated the surface property of fully amorphous particles prepared by spray-drying. We thus consider the milled particles used in this study (ML60, ML300 and ML1200) to be a type of core-shell particles with a partially disordered core containing defects and an amorphous shell (Bordet et al., 2016). The particle disorder in terms of apparent amorphous content (AAC) of the milled particles varied between about 10% and 80% (Table 1) which accordingly may be explained by an increased crystal defect density in the core and the formation of an amorphous shell. One should however note that the milled lactose powders used in this study are of complex nature, consisting of single particles and of particle agglomerates composed of very small particles adhered to the surface of larger particles (Pazesh et al., 2017). Spray-dried particles typically consist of an amorphous shell surrounding a void of air (Elversson et al., 2003), i.e. also the SDL particles are core-shell particles. In this paper, the tabletability and compactibility of this type of disordered core-shell particles is investigated and compared to crystalline particles of the same substance.

4.2. Tensile strength – compaction pressure relationships

It is earlier proposed (Alderborn, 2003) that the relationship between compact tensile strength and compaction pressure (tabletability) for many powders can be approximated with a three-stage model (Persson and Alderborn, 2018). In the first stage, no coherent compact is formed but above a critical formation pressure, a second stage is entered within which the compact tensile strength initially increases nearly linearly with pressure. In the end of the second stage, the relationship bends more or less sharply and a plateau is finally reached with a constant tensile strength independent of compaction pressure, representing the third stage. This stage is assumed to be associated with very low and nearly constant compact porosity. Deviations from this three-stage model in terms of a maximum (a peak) tensile strength followed by a steady reduction in strength with pressure are reported in the literature, e.g. (Osei-Yeboah et al., 2016). Some authors (Cole et al., 1975; Shotton and Ganderton, 1961) found that this drop coincided with an increased variation in tensile strength and explained the drop with lamination and cracking of the compacts. The drop in the relationship has also been explained (Osei-Yeboah et al., 2016; Sun, 2011) by elastic recovery and rupturing of inter-particulate bonds during decompression, a phenomenon denoted overcompaction by the authors. This three-stage model of a strength-pressure relationship could well describe the compaction properties of all powders (Figs. 1A and B) and compaction parameters that represent descriptors of the strength-pressure relationship were hence calculated, i.e. $\sigma_{t,\ max}$, k_c, P_{c1} and P_{c2}. In this study, the plateaus obtained for the strength-pressure relationship must be described as generally stable although in some cases a reduction in compact tensile strength was obtained at the highest applied pressures for both crystalline and disordered powders. The variation in compact tensile strength (Figs. 1A and B) was more or less independent of the applied compaction pressure. By inspection in a light microscope, no visible cracks could be observed on the surfaces of the compacts.

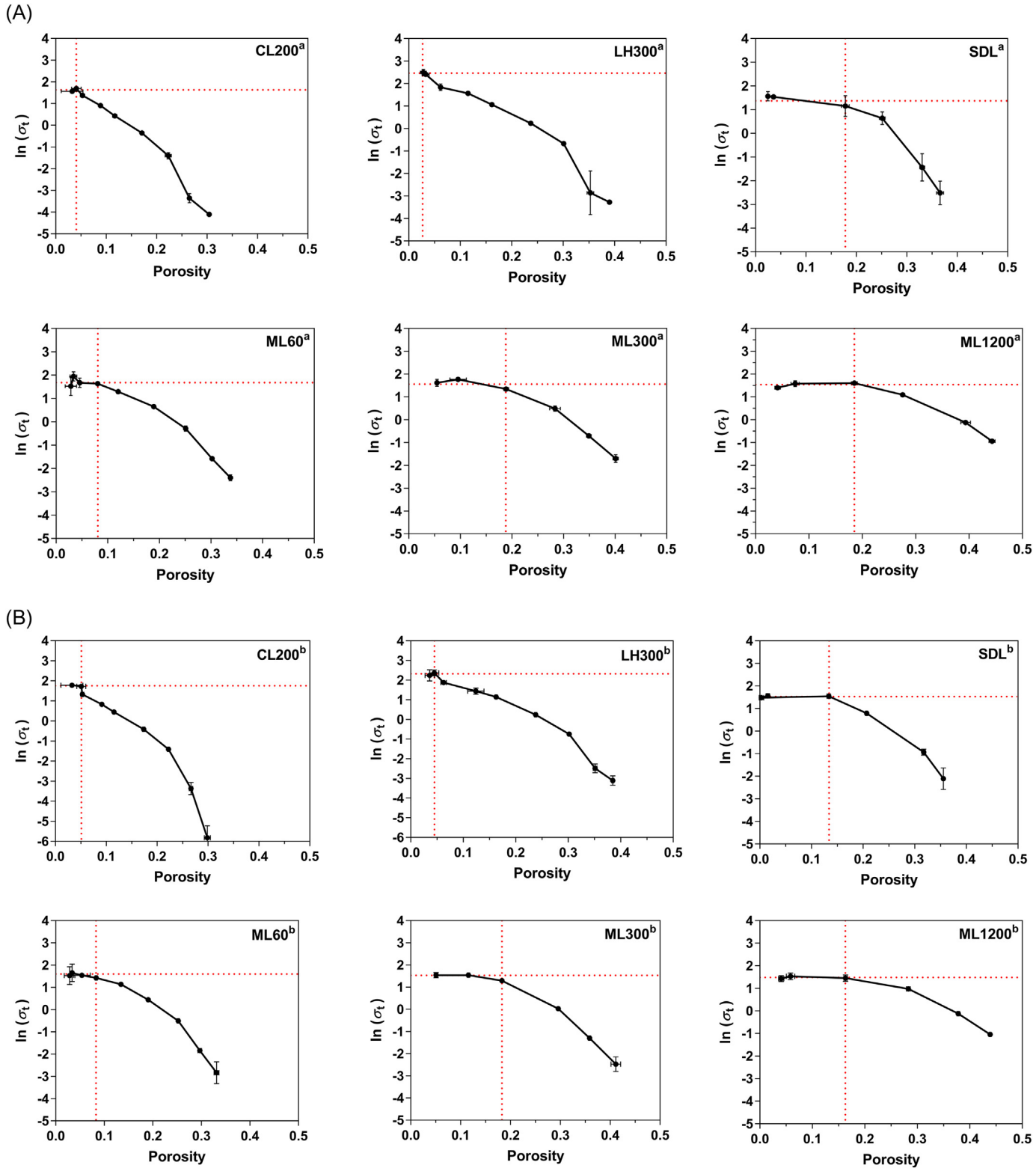

Fig. 3. The tensile strength (σ_t) and porosity relationship of crystalline lactose CL200, crystalline lactose LH300, lactose milled for 60 min (ML60), lactose milled for 300 min (ML300), lactose milled for 1200 min (ML1200) and spray-dried lactose (SDL) using Ryshkewitch-Duckworth model. Powder was pre-stored at 0% RH (A) and 33% RH (B) prior compaction. The red dashed horizontal line represents the maximum tensile strength ($\sigma_{t,\,max}$) and the red dashed vertical line represents the porosity at the $\sigma_{t,\,max}$. The error bars represent the standard deviations. (For interpretation of the references to colour in this figure legend, the reader is referred to the web version of this article.)

The character of the strength-pressure relationship was strongly dependent on both the original particle size of the crystalline materials (CL200 and LH300) and the degree of disorder of the powders (Figs. 1A and B), as shown also by the compaction parameters derived from the strength-pressure relationship, i.e. $\sigma_{t,\,max}$, k_c and P_{c2} (Figs. 2A, B and C). For the crystalline powders, the $\sigma_{t,\,max}$, k_c and P_{c2} were generally higher for LH300 than for CL200. It is earlier shown (Pazesh et al., 2018) that the median particle diameter of LH300 (3.46 μm) is markedly lower than for CL200 (27.4 μm). In accordance with earlier experience on the compaction properties of lactose powders (Vromans et al., 1985) the difference in tabletability between LH300 and CL200 is explained by the lower median particle size of the former. It is earlier shown (Pazesh et al., 2018) that the particle size distribution of LH300 is similar to the size distributions of the ML powders used in this study. Of this reason we consider LH300 as the relevant crystalline reference powder to the milled and disordered powders rather than CL200. Comparing the lactose powder of intermediate (ML300) and the powders of high degree of disorder (ML1200 and SDL) with the crystalline reference LH300 (Figs. 1 and B) markedly different tabletability plots were obtained. The lower k_c of LH300 display that the ML300, ML1200 and SDL powders formed tablets of higher strength due to their disordered character than LH300 at corresponding pressures. Furthermore, the P_{c2} decreased with increased milling time for the milled disordered powders and were markedly lower than for LH300 (Fig. 2C). We have earlier reported that the particle plastic stiffness of disordered powders during compression, as assessed by the Heckel parameter, decreased gradually with increased milling time and increased AAC, i.e. ML60 > ML300 > ML1200 (Pazesh et al., 2018). The particle plastic stiffness affects the evolution in inter-particulate specific contact area where less stiff particles have a higher propensity of forming large contact areas. Thus, it appears reasonable that the increased k_c for the disordered powders compared to LH300 was due to the decreased plastic stiffness caused by the disordering of the particles compared to for the crystalline powder LH300.

The ML60 powder, representing a powder of modest degree of disorder with an AAC of about 1–10%, had a strength-pressure relationship in-between the reference powders (Figs. 1A and B). The k_c was close to the crystalline reference, i.e. LH300, while the other compaction parameters were similar to the amorphous reference SDL (Figs. 1 and 2). One may note that the ML60 tended to recrystallise during pre-storage in the humid condition (RH 33%, Table 1) which changed the tabletability towards the crystalline reference. Thus, a more or less constant tabletability was obtained for the disordered particles from an AAC of about 25% and up-wards, i.e. similar k_c, $\sigma_{t,\,max}$ and P_{c2}. Hence, one may describe the effect of AAC on the tabletability of the powders used in this study as a step-wise effect with one compaction behaviour for crystalline particles and particles with a modest degree of disorder and one compaction behaviour for particles of intermediate and high degree of disorder.

The tabletability of a type of core-shell particle prepared by layering a shell on the core particles has earlier been studied by Sun et al. (Shi and Sun, 2011). It was reported that an increased shell thickness increased the compact forming ability of the powder. This was explained by an increasing area of contact formed between the particles with increasing shell thickness. The milled particles used in this study are considered to be core-shell particles. Among those, the ML60 particles formed compacts of a lower k_c than the other (ML300 and ML1200). An explanation is that the ML60 particles had a very thin disordered layer giving a relatively limited effect on the overall particle plastic stiffness and compact forming ability. The ML300 and ML1200 powders gave the same k_c although the AAC differed. One explanation is that the shell thickness became constant above a critical thickness and thus, the evolution of inter-particulate contacts was independent of AAC. Further disordering (increased AAC) was consequently caused by an increased defect density of the core (Bordet et al., 2016). An alternative explanation is that above a critical shell thickness the evolution of inter-particulate contacts was independent of shell thickness.

As stated above, the pre-storage humidity had generally a limited effect on the k_c for the disordered powders. It is earlier reported that the plastic stiffness of ML60 was increased after pre-storage in the humid atmosphere due to recrystallisation. The slight reduction in k_c after pre-storage in humid atmosphere (Fig. 2B) may consequently be explained by an increased particle plastic stiffness due to recrystallisation. It was further earlier reported that the plastic stiffness of the ML300 and ML1200 was not affected by pre-storage at 33% RH and these particles recrystallised only to a limited degree (Pazesh et al., 2018). The k_c of the ML300 and ML1200 can consequently be expected to be unaffected by the pre-storage humidity. In contrast, the plastic stiffness of SDL particles decreased after pre-storage in humid atmosphere and in this study, a tendency to a reduction in k_c after pre-storage in humid atmosphere was obtained (Fig. 2B). This is consistent with an earlier suggestion (Sebhatu et al., 1997) that sorbed moisture may plasticise amorphous particles and decrease their plastic stiffness and thus increase k_c. The lack of effect of pre-storage humidity on the k_c of the highly disordered ML300 and ML1200 is consequently unexpected, i.e. also for these powders sorbed moisture may potentially plasticise the particles. The limited effect of moisture content on the plastic stiffness and the k_c may be explained by the core-shell nature of the disordered particles. For such a particle, the amorphous shell may be plasticised but if the shell volume only represents a limited fraction of the particle volume, the effect of such a plasticisation on the plastic stiffness and the evolution of inter-particulate contacts may be limited. The consequence is that moisture sorbed into the defective core will not affect particle plastic stiffness.

4.3. Tensile strength-porosity relationships

It is earlier reported that the tensile strength-porosity relationships for a range of powders obey the Ryshkewitch-Duckworth equation (Adolfsson and Nyström, 1996; Etzler et al., 2011; Mishra and Rohera, 2019; Reynolds et al., 2017; Steendam and Lerk, 1998; Sun, 2005, 2016; Wu et al., 2006). The Ryshkewitch-Duckworth ability to describe strength-porosity relationships has been used as an argument for utilising this equation (Reynolds et al., 2017; Wu et al., 2005; Wu et al., 2006) to predict the compact forming ability of powder mixtures. To further investigate the effect of disordering on the decrease in the values of the compaction parameter P_{c2} compared to the crystalline reference, the tensile strength-porosity relationships were studied for all powders in accordance with the Ryshkewitch-Duckworth model. Generally, for all the investigated powders especially disordered ML and SDL powders, the tensile strength-porosity relationships deviated from the ideal Ryshkewitch-Duckworth relationship (Figs. 3A and B). Thus, the selection of a suitable porosity range for calculation of the compaction parameters i.e. the slope (k_R) and the tensile strength extrapolated to zero porosity (σ_0) is thus not evident and not meaningful. However, the Ryshkewitch-Duckworth plots can be categorised into two groups. The first group is represented by the crystalline powders and they are characterised by a steady, albeit not perfectly linear, increase in tablet tensile strength with reduced compact porosity. The Ryshkewitch-Duckworth plots for the crystalline powders were nearly linear from nearly zero porosity up to relatively high compact porosities, i.e. about 0.25. The second group is represented by the disordered powders and a characteristic feature of the Ryshkewitch-Duckworth plots for these powders was that the profiles bended markedly and a nearly constant compact tensile strength was obtained over a significant porosity range below a critical porosity (approximated by the red dashed lines in Figs. 3A and B). Thus, although the compact was densified, corresponding to a change in the compact micro-structure, no accompanying increase in tensile strength was obtained.

A marked deviation from the Ryshkewitch-Duckworth relationship has also earlier been reported (Jarosz and Parrott, 1982) and explained by a tendency for the low porosity compacts to cap. In that study, the

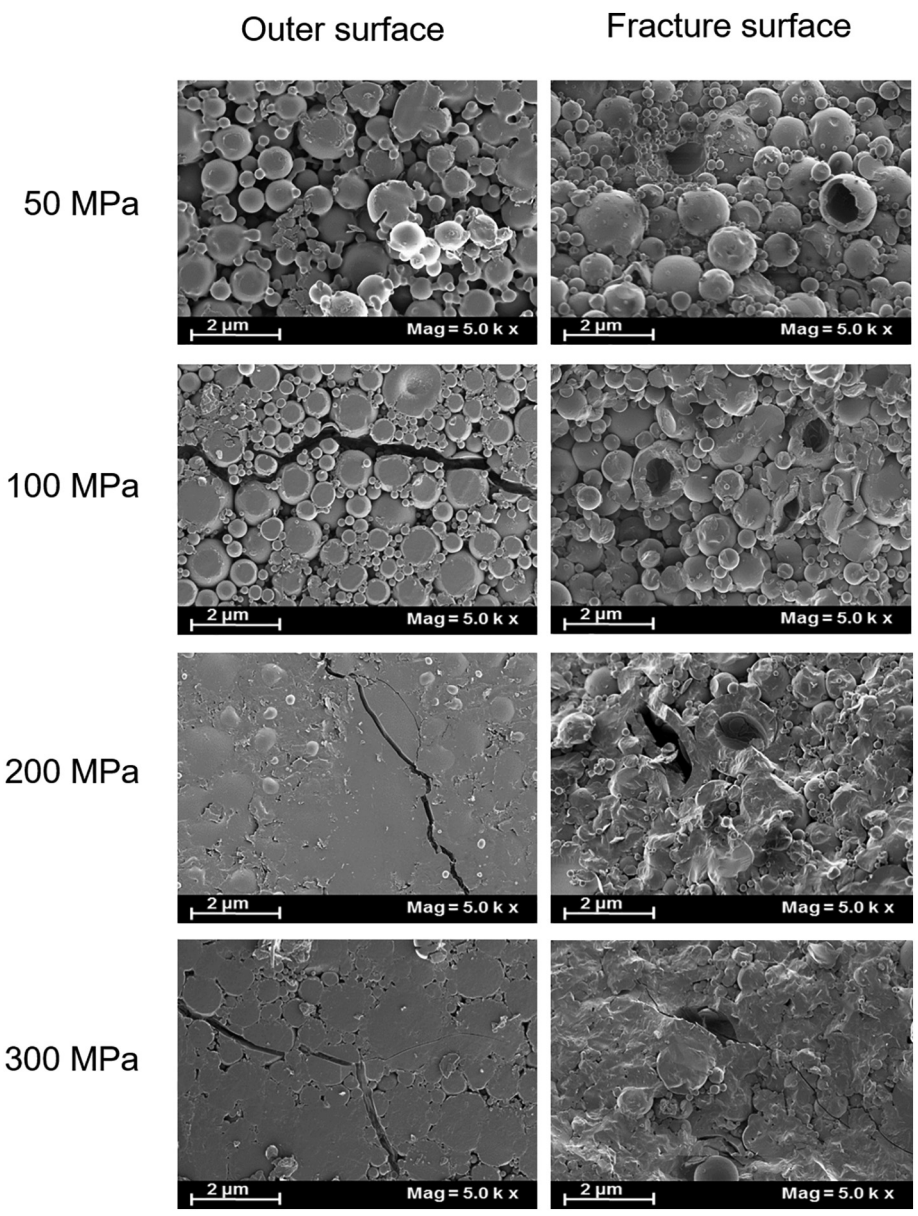

Fig. 4. SEM images of outer surface and fracture surface of compact fragments of spray-dried lactose. The powder was compacted at 50, 100, 200 and 300 MPa corresponding to a porosity of 0.25, 0.18, 0.04 and 0.03, respectively.

tensile strength was determined in the axial direction, i.e. parallel to the compaction direction, while in this study a standard approach to measure a tensile strength was used, also referred to as a radial tensile strength (Nyström et al., 1978).

4.4. Typical and atypical compaction behaviour

Based on the character of the tensile strength-porosity relationships, the compaction behaviour of the powders used in this study is categorised as either typical or atypical. The typical behaviour in this study is represented by the crystalline lactose powders while the atypical behaviour is represented by the disordered powders. For the disordered powders, a plateau in the compactibility plots were entered at porosities of about 0.15–0.20 and below this critical porosity, the powders compressed and densified over a relatively large range of porosities without an accompanying increase in compact tensile strength. Thus, although the sum of inter-particulate bonding forces acting over a cross-section of the compact probably increased due to densification, the actual stress required to break the compact was independent of compact porosity.

Irrespective of the type of compaction behaviour, i.e. typical and atypical, the tensile strength-pressure relationships for all powders could be approximated by the three-stage compaction model. As discussed above, the strength-pressure profiles obtained for the disordered particles showed a k_c that was higher than for the crystalline reference LH300 but the compaction parameters $\sigma_{t,\ max}$ and P_{c2} derived from the strength-pressure relationships decreased. The behaviour characterising the disordered powders, i.e. they compressed and densified over a relatively large range of porosities without an accompanying increase in compact tensile strength, explains the step-wise decrease in values of the compaction parameters $\sigma_{t,\ max}$ and P_{c2} of these powders.

Solid bodies break by a kinematic process, i.e. the fracture will be initiated at some weak part of the specimen, often referred to as a flaw, and propagate across the failure surface. In the literature (Rice, 1984; Shotton and Ganderton, 1961), two types of failure of a compact has been proposed, i.e. a failure between the particles forming the compact (referred to as around grain type of failure) and a failure through the particles forming the compact (referred to as across grain type of

failure). It is reasonable that the strength of a compact of relatively high porosity depends on the force needed to break the inter-particulate bonds, i.e. the fracture propagates along the inter-particulate junctions (around grain failure). The property controlling the strength of the compact is consequently the sum of the inter-particulate bonds across the fracture surface. However, with decreasing porosity the bonding forces between the particles will increase and a situation may eventually be approached where the force needed to break the inter-particulate bonds approximates the force needed to break the particles forming the compact. The property controlling the strength of the compact may then be approximated by the strength of the particles.

It is logical that if the rate of change in tensile strength with porosity is constant (k_R), the property controlling the strength of the compact is the same. It is proposed (Etzler et al., 2011) that the k_R represents an indication of the propensity of the particles to develop areas of inter-particulate contact during compression which presumably controls the strength of the compact. A modification in the rate of change in tensile strength with porosity indicates consequently that the property controlling the strength is altered. It is thus possible that the atypical compaction behaviour observed for the disordered particles used in this study is due to that a shift in compact fracture pattern occurs at a porosity (indicated by the vertical dashed lines in Figs. 3A and B) considerably higher than for compacts of crystalline lactose showing a typical compaction behaviour. As a means to investigate the fracture pattern occurring at various porosity of compacts formed of disordered particles, images were prepared by SEM of outer and fracture surfaces of compact fragments. Since crystalline and milled particles are irregular and rough, it is difficult to distinguish between around and across grain fracture pattern for compacts of such particles. However, preparation of disordered particles by spray-drying gave relatively spherical and smooth particles of core-shell nature and the SDL powder was hence chosen for studying the fracture pattern of compacts of different porosity. Compacts were prepared at four compaction pressures (50, 100, 200 and 300 MPa) resulting in varying compact porosities ranging from high (50 MPa compaction pressure) to low (200 and 300 MPa compaction pressures) i.e. located in the linear region and in the plateau region of the log-lin strength-porosity relationship, respectively. The 100 MPa compaction pressure resulted in a compact porosity at which the plateau was entered and this compact porosity represented an intermediate stage between the linear region and the plateau region of the log-lin strength-porosity relationship.

In general, the compacts could be described as large agglomerates of amorphous lactose particles and an increased compaction pressure gave compacts with a more closed pore structure (Fig. 4). At high compact porosity (50 MPa compaction pressure) relatively weak compacts were formed and the SDL particles were only slightly deformed and the inter-particulate voids were relatively large. The fracture of the compact appeared to occur primarily at the inter-particle junctions. At intermediate porosity (100 MPa compaction pressure) the particles were more deformed and the inter-particulate voids reduced and a more closed pore structure was thus obtained compared to the high porosity compact. The fracture of the compact occurred predominantly at the inter-particulate junctions during strength testing albeit intra-particulate failure occurred to a limited degree, i.e. cleaved particles could be observed along the fracture both at the compact surface and at the fracture surface. At low compact porosities (200 and 300 MPa compaction pressures), i.e. strong compacts, the particles were more deformed and the void size markedly reduced. Furthermore, it appeared that the compact fracture pattern shifted from occurring predominantly around to across the primary particles. It is thus concluded that the dominating type of compact fracture pattern changed with reduced compact porosity, from around to across grain fracture, and that this change occurred approximately when the plateau part of the Ryshkewitch-Duckworth plot was entered, i.e. at compact porosities of about 0.1 for the SDL powder. It is thus proposed that the change of dominating type of compact fracture pattern explains the type of compaction behaviour referred to as atypical.

The type of disordered particles (ML and SDL powders) used in this study can be described as core-shell particles with a shell consisting of amorphous solid. For the SDL particles, the hollow core corresponds to the defective core of the milled particles. Thus, the same reasoning to explain the atypical compaction behaviour of the SDL particles is proposed to be valid also to explain the atypical behaviour of the milled particles.

For a powder showing a typical compaction behaviour, the rate of change in tensile strength with porosity is nearly constant down to a porosity of nearly zero indicating the same underlying strength controlling property of the compact. It is proposed that this property is the inter-particulate bond network and the tablet fails predominantly by an around grain type of failure. For a powder showing an atypical compaction behaviour, the rate of change in tensile strength with porosity ceased at a critical porosity and this coincided with a change in dominating type of compact failure, i.e. from around to across grain type of failure. Thus, while loaded the fracture may propagate across the particles rather than by finding its way around the particles.

This indicates a change in the strength-controlling property of the compact and it is proposed that the strength-controlling property change from the inter-particulate bond network (before entering the plateau) to the particle strength (at the plateau).

This conceptual discussion of the strength-controlling property of a compact accentuates the question of the physical significance of the extrapolated tensile strength value (σ_0). Different explanations for the physical meaning of σ_0 is proposed in the literature (Olsson et al., 1996), i.e. the intrinsic bond strength of the material, the strength of the particles forming the compact and an indication of the inter-particulate bond strength. In this study, an effect of the initial particle size on the extrapolated tensile strength was obtained (LH300 versus CL200), supporting an earlier conclusion (Adolfsson et al., 1997) that the extrapolated tensile strength does not represent an intrinsic material strength. As a consequence of the conceptual reasoning above it is here proposed that the σ_0 may represent either an indication of the particle strength or of the inter-particulate bond strength dependent on their relation (Shotton and Ganderton, 1961). For powders showing typical compaction behaviour, σ_0 represents a finite indication of the strength of the inter-particulate bond network while for powders showing atypical compaction behaviour, σ_0 reflects an effective particle strength. For the materials used in this study, the highest σ_0 was obtained for LH300 (Fig. 3). This powder is here categorised as showing typical compaction behaviour and σ_0 represents hence a finite indication of the strength of the inter-particulate bond network. The high strength of the inter-particulate bond network for LH300 can be explained by the combined effect of a low initial particle diameter, providing condition for a large specific number of inter-particulate contact points in the compact, and a pronounced plastic deformation of the particles during powder compression, resulting in a substantial area of contact at each particle-particle contact site. For a powder showing typical compaction behaviour, the tablet fractures predominantly by an around grain type of failure. The absence of significant across grain failure may be explained by a high strength of the particles forming the compact, which is reasonable for LH300 due to the very low particle diameter of this lactose quality.

5. Conclusion

In this paper, the compaction behaviour of disordered lactose particles prepared by milling and by spray-drying was compared to the compaction behaviour of two crystalline lactose powders. The compaction behaviour was strongly dependent on the apparent amorphous content of the particles in an intricate way as follows:

- The compaction behaviour changed in a step-wise way with increasing apparent amorphous content and was hence categorised

into two groups, referred to as typical and atypical compaction behaviour. The typical behaviour was shown by the crystalline lactose powders while the atypical behaviour was shown by the disordered powders.

- The terms typical and atypical are used to describe the character of the compact tensile strength-porosity relationships (compactibility) expressed according to the Ryshkewitch-Duckworth expression. The typical compaction behaviour is characterised by a steady, albeit not perfectly linear, increase in tablet tensile strength with reduced compact porosity down to a porosity of nearly zero while the converse applied for the atypical behaviour. The characteristic feature of the atypical behaviour was that over a considerable range of low compact porosities, a reduction in compact porosity gave not an accompanying increase in tensile strength, i.e. a plateau in the tensile strength-porosity profile was obtained. The transition in rate of change in compact tensile strength with porosity is explained by a shift in the dominating type of fracture behaviour of the compact during strength testing, from occurring predominantly around to predominantly across the primary particles. Thus, this shift reflects a change in the property which controls the strength of the compact, from the inter-particulate bond structure to the strength of the particles forming the compact.
- The tensile strength-compaction pressure relationship (tabletability) of the powders followed the three-stage compaction model and compaction parameters could be determined. The disordered particles showed an initial higher gradient of the relationship compared to the crystalline powders, explained by an increased particle plasticity due to the disordering. However, the maximal compact tensile strength and the compaction pressure at which the strength plateau was reached were lower for the disordered particles, explained by the shift in the strength controlling type of fracture pattern of the compact, i.e. from around grain to across grain.

The results of the compaction study also sheds light on the process of disordering of lactose particles during milling. The milled particles can be described as a type of core-shell particles with an amorphous shell and a partially disordered core. The amorphous shell seems to be formed early in the milling process and has thereafter a nearly constant thickness with increased milling time. Thus, the increase in apparent amorphous content occurring during milling subsequent to the formation of the amorphous layer is explained by an increased degree of disorder of the core due to the formation of defects and fragmentation of crystallites. The nature of the milled particles are thus complex and seems to consist of both an amorphous and a defective phase.

Declaration of competing interest

None.

Acknowledgments

The authors wish to thank Prof. Peter Lazor, Department of Earth Sciences, Mineralogy Petrology and Tectonics, Uppsala University, Sweden, for providing the Raman instrument used in this research. The authors thank Dr. Lucia Lazorova for skilful preparation of SEM images.

References

Adolfsson, A., Nyström, C., 1996. Tablet strength, porosity, elasticity and solid state structure of tablets compressed at high loads. Int. J. Pharm. 132, 95–106.
Adolfsson, Å., Olsson, H., Nyström, C., 1997. Effect of particle size and compaction load on interparticulate bonding structure for some pharmaceutical materials studied by compaction and strength characterisation in butanol. Eur. J. Pharm. Biopharm. 44, 243–251.
Alderborn, G., 2003. A novel approach to derive a compression parameter indicating effective particle deformability. Pharm. Dev. Technol. 8, 367–377.
Alderborn, G., Nyström, C., 1982. Studies on direct compression of tablets. IV. The effect of particle size on the mechanical strength of tablets. Acta Pharmaceutica Suecica 19, 381–390.
Badal Tejedor, M., Nordgren, N., Schuleit, M., Pazesh, S., Alderborn, G., Millqvist-Fureby, A., Rutland, M.W., 2017. Determination of interfacial amorphicity in functional powders. Langmuir 33, 920–926.
Bordet, P., Bytchkov, A., Descamps, M., Dudognon, E., Elkaïm, E., Martinetto, P., Pagnoux, W., Poulain, A., Willart, J.-F., 2016. Solid state amorphization of β-trehalose: a structural investigation using synchrotron powder diffraction and PDF analysis. Cryst. Growth Des. 16, 4547–4558.
Cole, E.T., Rees, J.E., Hersey, J.A., 1975. Relations between compaction data for some crystalline pharmaceutical materials. Pharm. Acta Helv. 50, 28–32.
Duckworth, W., 1953. Discussion of ryshkewitch paper. J. Am. Ceram. Soc. 36, 68.
Dujardin, N., Willart, J.F., Dudognon, E., Danède, F., Descamps, M., 2013. Mechanism of solid state amorphization of glucose upon milling. J. Phys. Chem. B 117, 1437–1443.
Elversson, J., Millqvist-Fureby, A., Alderborn, G., Elofsson, U., 2003. Droplet and particle size relationship and shell thickness of inhalable lactose particles during spray drying. J. Pharm. Sci. 92, 900–910.
Etzler, F.M., Bramante, T., Deanne, R., Sienkiewicz, S., Chen, F.J., 2011. Tablet tensile strength: an adhesion science perspective. J. Adhes. Sci. Technol. 25, 501–519.
Fell, J.T., Newton, J.M., 1970. Determination of tablet tensile strength by the diametral-compression test. J. Pharm. Sci. 59, 688–691.
Jarosz, P.J., Parrott, E.L., 1982. Factors influencing axial and radial tensile strengths of tablets. J. Pharm. Sci. 71, 607–614.
Luisi, B.S., Medek, A., Liu, Z., Mudunuri, P., Moulton, B., 2012. Milling-induced disorder of pharmaceuticals: one-phase or two-phase system? J. Pharm. Sci. 101, 1475–1485.
Mishra, S.M., Rohera, B.D., 2019. Mechanics of tablet formation: a comparative evaluation of percolation theory with classical concepts. Pharm. Dev. Technol. 1–13.
Newman, A., Zografi, G., 2014. Critical considerations for the qualitative and quantitative determination of process-induced disorder in crystalline solids. J. Pharm. Sci. 103, 2595–2604.
Nyström, C., Malmqvist, K., Mazur, J., Alex, W., Holzer, A.W., 1978. Measurement of axial and radial tensile strength of tablets and their relation to capping. Acta Pharm. Suec. 15, 226–232.
Nyström, C., Alderborn, G., Duberg, M., Karehill, P.-G., 1993. Bonding surface-area and bonding mechanism-two important factors for the understanding of powder compactibility. Drug Dev. Ind. Pharm. 19, 2143–2196.
Olsson, H., Adolfsson, Å., Nyström, C., 1996. Compaction and measurement of tablets in liquids with different dielectric constants for determination of bonding mechanisms—Evaluation of the concept. Int. J. Pharm. 143, 233–245.
Osei-Yeboah, F., Chang, S.Y., Sun, C.C., 2016. A critical examination of the phenomenon of bonding area - bonding strength interplay in powder tableting. Pharm. Res. 33, 1126–1132.
Pazesh, S., Lazorova, L., Berggren, J., Alderborn, G., Grasjö, J., 2016. Considerations on the quantitative analysis of apparent amorphicity of milled lactose by Raman spectroscopy. Int. J. Pharm. 511, 488–504.
Pazesh, S., Gråsjö, J., Berggren, J., Alderborn, G., 2017. Comminution-amorphisation relationships during ball milling of lactose at different milling conditions. Int. J. Pharm. 528, 215–227.
Pazesh, S., Persson, A.-S., Berggren, J., Alderborn, G., 2018. Effect of milling on the plastic and the elastic stiffness of lactose particles. Eur. J. Pharm. Sci. 114, 138–145.
Persson, A.-S., Alderborn, G., 2018. A hybrid approach to predict the relationship between tablet tensile strength and compaction pressure using analytical powder compression. Eur. J. Pharm. Biopharm. 125, 28–37.
Reynolds, G.K., Campbell, J.I., Roberts, R.J., 2017. A compressibility based model for predicting the tensile strength of directly compressed pharmaceutical powder mixtures. Int. J. Pharm. 531, 215–224.
Rice, R.W., 1984. Pores as fracture origins in ceramics. J. Mater. Sci. 19, 895–914.
Ryshkewitch, E., 1953. Compression strength of porous sintered alumina and zirconia. J. Am. Ceram. Soc. 36, 65–68.
Sebhatu, T., Alderborn, G., 1999. Relationships between the effective interparticulate contact area and the tensile strength of tablets of amorphous and crystalline lactose of varying particle size. Eur. J. Pharm. Sci. 8, 235–242.
Sebhatu, T., Ahlneck, C., Alderborn, G., 1997. The effect of moisture content on the compression and bond-formation properties of amorphous lactose particles. Int. J. Pharm. 146, 101–114.
Shi, L., Sun, C.C., 2011. Overcoming poor tabletability of pharmaceutical crystals by surface modification. Pharm. Res. 28, 3248–3255.
Shotton, E., Ganderton, D., 1961. The strength of compressed tablets. III. The relation of parcticle size, bonding and capping in tablets of sodium chloride, aspirin and hexamine. J. Pharm. Pharmacol. 13 (Suppl), 144–152.
Steendam, R., Lerk, C.F., 1998. Poly(dl-lactic acid) as a direct compression excipient in controlled release tablets: part I. Compaction behaviour and release characteristics of poly(dl-lactic acid) matrix tablets. Int. J. Pharm. 175, 33–46.
Sun, C.C., 2005. Quantifying errors in tableting data analysis using the Ryshkewitch equation due to inaccurate true density. J. Pharm. Sci. 94, 2061–2068.
Sun, C.C., 2011. Decoding powder tabletability: roles of particle adhesion and plasticity. J. Adhes. Sci. Technol. 25, 483–499.
Sun, C.C., 2016. A classification system for tableting behaviors of binary powder mixtures. Asian J. Pharmac. Sci. 11, 486–491.
Tye, C.K., Sun, C.C., Amidon, G.E., 2005. Evaluation of the effects of tableting speed on the relationships between compaction pressure, tablet tensile strength, and tablet solid fraction. J. Pharm. Sci. 94, 465–472.
Vromans, H., Deboer, A.H., Bolhuis, G.K., Lerk, C.F., Kussendrager, K.D., 1985. Studies on tabletting properties of lactose I. the effect of particle-size on binding properties and dehydration characteristics of lactose. Acta Pharmaceutica Suecica 22, 163–172.
Vromans, H., Bolhuis, G.K., Lerk, C.F., van de Biggelaar, H., Bosch, H., 1987. Studies on tableting properties of lactose. VII. The effect of variations in primary particle size

and percentage of amorphous lactose in spray dried lactose products. Int. J. Pharm. 35, 29–37.
Wu, C.-Y., Best, S.M., Bentham, A.C., Hancock, B.C., Bonfield, W., 2005. A simple predictive model for the tensile strength of binary tablets. Eur. J. Pharm. Sci. 25, 331–336.
Wu, C.Y., Best, S.M., Bentham, A.C., Hancock, B.C., Bonfield, W., 2006. Predicting the tensile strength of compacted multi-component mixtures of pharmaceutical powders. Pharm. Res. 23, 1898–1905.